Письма в ЖЭТФ, том 78, вып. 6, с. 845 – 849 © 2003 г. 25 сентября

Structural transformations in liquid, crystalline and glassy B_2O_3 under high pressure

V. V. Brazhkin[1)], *Y. Katayama*[+], *Y. Inamura*[+], *M. V. Kondrin, A. G. Lyapin, S. V. Popova, R. N. Voloshin*

Institute for High Pressure Physics RAS, 142190 Troitsk, Moscow reg., Russia

[+]*Japan Atomic Energy Research Institute SPRING 8, 1-1-1 Kouto Mikazuki, Sayo, Hyogo, 679-5143, Japan*

Поступила в редакцию 19 августа 2003 г.

We present *in situ* (X-ray diffraction) and *ex situ* (quenching) structural study of crystalline, liquid, and glassy B_2O_3 up to 9 GPa and 1700 K, drawing equilibrium and non-equilibrium phase diagrams of B_2O_3. Particularly, we have determined the melting curve, the stability regions for crystalline B_2O_3 I and B_2O_3 II modifications, the regions of transformations, such as densification or crystallization, for both the liquid and glassy states, including the region of sharp first-order–like transition in liquid B_2O_3 to a high-density phase nearby 7 GPa. Quenching experiments also show that the transition to the high-density liquid can occur at much lower pressures in non-stochiometric melt with excess of boron. B_2O_3 is the first glassformer, where transformations in the disordered state have been comparatively studied for both liquid and glassy phases.

PACS: 61.20.−p, 61.43.−j, 62.50.+p, 64.70.−p

1. In contrast to phase transitions in crystals, transformations in disordered condensed media, such as liquids and glasses, have not been adequately studied to date at broad variations of temperature and pressure [1]. There are very few examples of disordered substances with the sharp structural changes and thermodynamic anomalies under pressure, e.g., the melts of P, Se, Bi, and Te, supercooled melts of Si and Ge, supercooled water and amorphous ices [1], which could be clear associated with transformations, similar or equivalent to the first-order transitions. For the amorphous ice H_2O [2] and liquid phosphorus [3] the macroscopic mixture of two amorphous or liquid phases, respectively, was observed at the transformation, that is the direct evidence for the first-order phase transition. However, in the majority of simple liquids, such as melts of alkali metals, and in ordinary glasses, such as a-SiO_2 and a-GeO_2, broad transformations between two disordered states are observed under pressure [1, 4, 5]. Only for H_2O ice and water the structural changes in liquid and disordered solid states are clearly compared (e.g., see [1] and references therein). For glassforming substances, there are still no examples of simultaneous comparative studies of phase transformations in the liquid and glassy states, due to high melting temperatures of readily glassforming substances, like SiO_2 and GeO_2 and, on the other hand, due to low stability temperatures of elementary amorphous substances and glasses based on P, Se, Bi, and Te.

In the present work, boron oxide B_2O_3 is chosen for study of transformations in the disordered media. This substance easily vitrifies and, at the same time, has low melting temperature $T_m \approx 750$ K at normal pressure. The melt and glass of B_2O_3 have the network structures, that in many respects makes them similar to archetypical glasses and melts, such as SiO_2 and H_2O [6]. Stable B_2O_3 I crystalline phase ($P3_1$ space group, $a = 4.336$ Å, $c = 8.340$ Å, and density $\rho \approx \approx 2.55$ g/cm^3) has the structure consisting of "ribbons" formed by B_2O_3 triangles [7]. The denser B_2O_3 II phase (space group $Ccm2_1$, $a = 4.613$ Å, $b = 7.803$ Å, $c = 4.129$ Å, and $\rho \approx 3.11$ g/cm^3 at normal conditions) with the orthorhombic structure, based on distorted BO_4 tetrahedrons, can be synthesized at high pressures ($P > 4$ GPa) and temperatures ($T > 1000$ K) [8]. The threefold boron coordination 3 (by oxygen) and the twofold oxygen coordination of 2 (by boron) in B_2O_3 I are changed to 4 and to the intermediate between 2 and 3, respectively, in B_2O_3 II [7, 8]. The pressure-temperature phase diagram of B_2O_3, including relative stability of these phases and the melting curve, has been rather scanty studied up to date [9 – 11]. Ordinary B_2O_3 glass is obtained from melt at very low cooling rates. This glass has the opened structure and low-density $\rho \approx 1.85$ g/cm^3 [6]. It is believed that the structure of this glass is based on low-coordinated boron atoms ($Z = 3$) and has a considerable fraction ($\sim 20\%$) of ring-shaped boroxol groups B_3O_6 [6, 11, 12]. The high-pressure treatment of B_2O_3 glass and quenching from melt under pressure allow one to obtain denser glasses

[1)] e-mail: brazhkin@hppi.troitsk.ru

with densities by 10 to 20% higher than ordinary values [11, 13]. At normal pressure the densified glasses relax to the normal state at 300 to 600 K, depending on the history of its preparation [11, 13]. The study of the structure of the B_2O_3 densified glasses suggested that the densification was mainly associated with the breakup of boroxol groups and buckling of "ribbons" formed by B_2O_3 triangles [14, 15].

There are quite a few studies concerning the temperature dependence of the structure of B_2O_3 glasses and liquids [16, 17]. The molecular dynamic simulation of the B_2O_3 points to a possibility of structural coordination changes in the melt under pressure and acceleration of self-diffusion in the melt during compression [18]. Recently we have got the indirect experimental evidence for decrease of viscosity and corresponding increase of diffusion in B_2O_3 melt under pressure [19]. The Raman and Brillouin study of B_2O_3 glass has been performed up to 14 GPa at room temperature [20, 21]. However, up to date there were no *in situ* studies of the structures of liquid, glassy, and even crystalline B_2O_3 under pressure.

The purpose of the present work is the *in situ* high-pressure X-ray study of liquid, glassy, and crystalline B_2O_3, supporting by quenching experiments, in order to study possible structural changes and phase transitions, to compare the behaviors of liquid and glassy states, to attain insight into the nature of B_2O_3 glass densification, and to examine the equilibrium and nonequilibrium phase diagrams of B_2O_3.

2. B_2O_3 ordinary glass, crystalline B_2O_3 I, and B_2O_3 II modifications (the last was specially obtained under pressure) were used as the starting phases for *in situ* experiments. Commercially available original B_2O_3 glasses contain, as a rule, several percents of H_2O in the bound state (e.g., in H_3BO_3). Heat treatment of B_2O_3 glass at $T \approx 600$–700 K during 20 to 30 hours or at $T \approx$ $\approx$ 800 K during 5 to 10 hours made it possible to obtain dehydrated specimens that were rapidly ($<$ 1 min) mounted into a high-pressure cell. The cylindrical specimens with diameter of 2 to 3 mm and height of 1 to 3 mm were placed into containers from BN, Pt, or Ta or directly into a graphite heater. Hermetic thick-wall Pt ampoules were used for the very high-temperature experiments ($>$ 1700 K) to avoid the partial decomposition of B_2O_3 compound and oxygen leakage. The "toroid" high-pressure chambers were used for the synthesis of crystalline phases and dense glasses, as well as for thermodynamic study by the differential thermal and thermo-baric analysis (DTA and TBA) up to 8 GPa and 2100 K. *in situ* structural experiments were carried out at the cubic multianvil press using the X-ray dispersive method (Spring-8, MAX-80 press, BL14B1 Beamline). The melt, crystalline phases, and glasses of B_2O_3 were studied to 5 GPa at high temperatures up to 1700 K and to 9 GPa at room temperature. The *in situ* X-ray diffraction patterns were obtained in 11 pressure-temperature points for liquid B_2O_3, in 44 points for glassy B_2O_3, and in almost 100 points for the B_2O_3 I and B_2O_3 II crystalline phases. The structure of quenched glasses at normal pressure was studied by X-ray diffraction (Bruker AXS). The density of the glasses was measured by the bottle method and by sinking the dense liquid mixtures. The hardness was measured using the PMT-3M microhardness tester. The index of refraction was studied by the immersion technique. The details of high-pressure experiments will be presented elsewhere.

3. The equilibrium phase diagram of B_2O_3 (Fig.1) is one of the main results of this study.

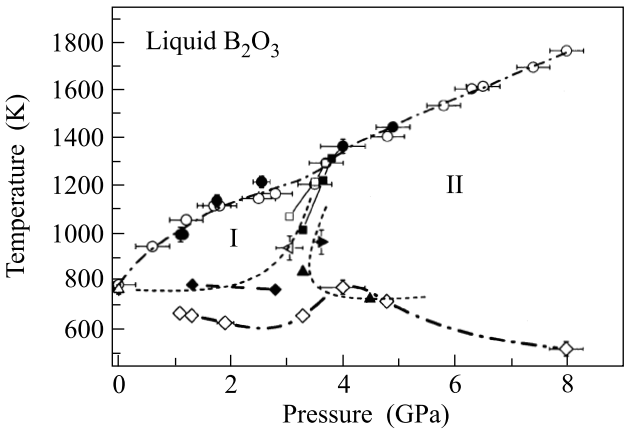

Fig.1. The pressure-temperature phase diagram of B_2O_3, where symbols correspond to experimental points and lines are interpolations. The melting curve is shown by solid (*in situ* study) and open (DTA, TBA, and quenching experiments) circles and dashed-dotted line; the crystallization line (for times of the order of several minutes) of compressed ordinary glass – by open diamonds and thick dashed-dotted line; the crystallization line of quenched at high pressure glasses – by solid diamonds and thick dashed line; the I→II and II→I kinetic transition lines – by solid and open, respectively, triangles and thin dashed lines, where orientation of the triangle shows the direction of movement on the pressure-temperature plane. Open and solid squares correspond to points, where I and II crystalline phases, respectively, do not transit to each other, i.e., are experimentally stable nearby the triple point I – II-melt. When experimental bar is not shown, it is comparable or less than the size of the symbol

The positions of the melting curve and I-II transition line established here noticeably differ from those on

the earlier versions of the phase diagram [9, 10]. We were the first who *in situ* observed the II→I transition in crystalline B_2O_3 during pressure release at high temperatures, that unambiguously confirms that B_2O_3 II is thermodynamically a high-pressure phase. Analysis of the *in situ* diffraction patterns for the crystalline phases allowed us to estimate their bulk moduli, $B \approx 55 \pm 15$ GPa for B_2O_3 I and $B \approx 90 \pm 15$ GPa for B_2O_3 II, and their expansion coefficients, $\alpha \approx (2 \pm 0.5) \cdot 10^{-5}\,K^{-1}$ for the both phases.

4. The *in situ* measured temperature of crystallization of the compressed ordinary B_2O_3 glass has a maximum at the pressures of 3.5 to 4.5 GPa (Fig.1), which is possibly related to the attainment of a rigid and unstressed glassy state [22]. The activation energy for the glass crystallization process at $P = 1.3$ GPa is $E_{act} \approx 120 \pm 15$ kJ/mole. The crystallization temperatures of glasses prepared by quenching from melt under high pressure exceeds by 100 to 150 K those for compressed pristine ordinary glass (Fig.1), indicating that the quenched high-pressure glasses are closer to the quasi-thermodynamic equilibrium state of glass at the corresponding pressures.

5. The typical X-ray diffraction patterns for the B_2O_3 glasses and liquid are shown in Fig.2. The *in situ* structural study of liquid B_2O_3 displays diffuse transformation under pressure within the 0.5 to 2.5 GPa range, that is clearly supported by a noticeable growth of the residual densification of glasses, obtained by quenching from melt (Fig.3a and b). The compressed ordinary B_2O_3 glass reveals at room temperature noticeable partially irreversible changes of the short-range order structure (Fig.2*a* and *b*), and the residual densification of quenched samples starts at pressure 5 to 6.5 GPa. At elevated temperatures $T > 500$ K these irreversible changes start at 1 to 1.5 GPa. A comprehensive analysis of the structural data with the calculation of the radial distribution functions will be presented elsewhere.

The unusual pressure dependence of the position of first X-ray diffraction peak at 3 to 5 GPa in the B_2O_3 liquid (Fig.3c) shows that besides the diffuse structural transformation at 0.5 to 2.5 GPa, one more liquid-liquid structural transformation is possible at higher pressures. To check this suggestion we studied the structure and properties of B_2O_3 glasses prepared by quenching from melt at 1 to 7.5 GPa. The glasses obtained at 4.5 to 6.5 GPa have the density $\rho \approx 2.2$–$2.4\,g/cm^3$, whereas the glasses obtained at $P > 7$ GPa have the density 2.8–$2.9\,g/cm^3$, which exceeds the density of original glass by 55% (Fig.3a). The X-ray diffraction study of these high-density glasses (Fig.2*e*) points to

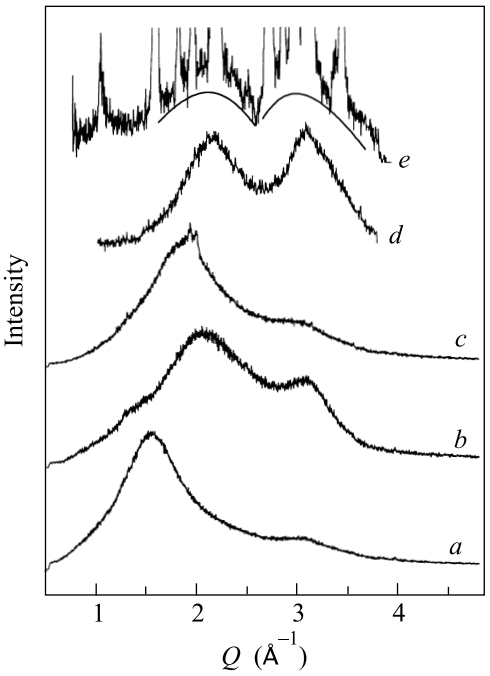

Fig.2. X-ray diffraction patterns for the ordinary B_2O_3 glass at $P = 10^{-4}$ GPa and $T = 300$ K (*a*), compressed ordinary glass at 8.42 ± 0.07 GPa and 300 K (*b*), liquid B_2O_3 at 4.0 ± 0.4 GPa and 1460 ± 20 K (*c*), high-density non-stochiometric glass with the composition $B_2O_{2.6}$ quenched from the B_2O_3-based melt at 5.7 ± 0.4 GPa 1800 ± 100 K in graphite container (*d*), and high-density stochiometric B_2O_3 glass mixed with new crystalline phase (its reflections are cut of), where the sample was quenched from the melt at 7.0 ± 0.5 GPa and 1900 ± 100 K in thick Pt container (*e*)

substantial changes in the short-range order structure (Fig.3d). Taking into account the compressibility of the glasses and their thermal expansion, it is possible to estimate the position of first X-ray diffraction peak for the corresponding melts (Fig.3d). The decrease of B_2O_3 melt viscosity under pressure [19] results in the formation of the crystal-glass mixture during quenching (10^3 K/s) instead pure glass at $P > 4.5$ GPa. At 4.5 to 6 GPa the mixture of both crystalline modifications B_2O_3 I and B_2O_3 II together with glass was formed after rapid cooling whereas at higher pressures the densest modification B_2O_3 II with small part of glass admixture was obtained after melt quenching. The data obtained for the structure and density of the highly densified B_2O_3 glass strongly evidence for the existence of one more sharp phase transition in liquid B_2O_3 at $P \approx 7 \pm 0.5$ GPa, accompanied by the volume anomaly $\Delta V/V \approx 20\%$ and a change in the short-range order structure. The high-density glass has a rather high index of refraction (Fig.3b), $n \approx 1.61$–1.63 (original glass

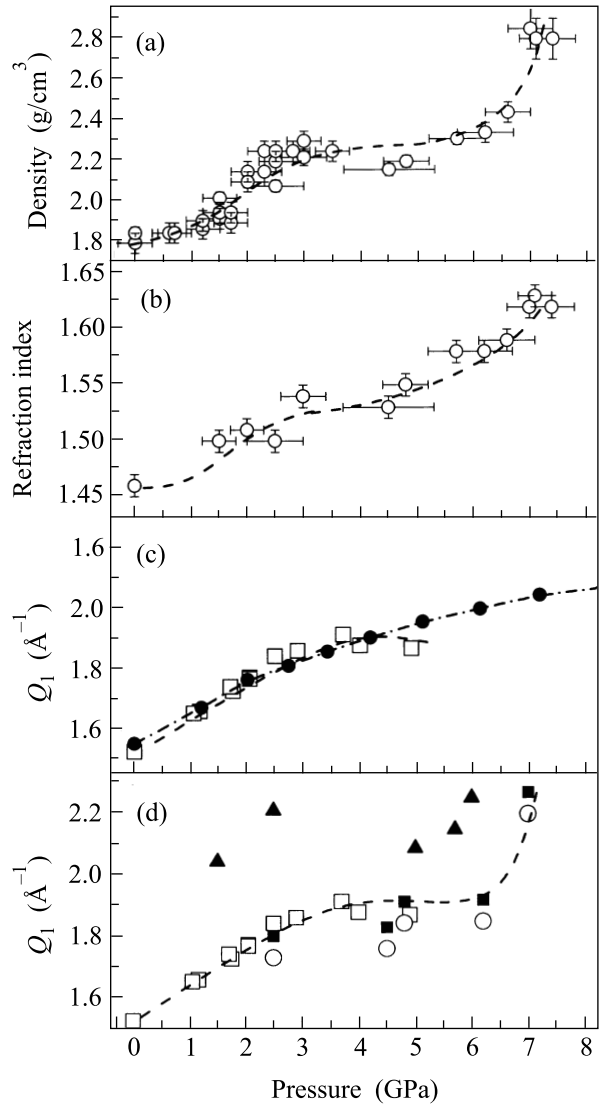

Fig.3. Density (a) and refractive index (b) for B_2O_3 glasses quenched from the melt and position of first X-ray diffraction peak for different cases ((c) and (d)) as functions of *in situ* pressure or pressure, from which the sample was quenched (depending on the comments). (c) The *in situ* data for liquid near melting curve (open squares) and for compressed ordinary glass (solid circles) are compared. (d) The same data for liquid B_2O_3 as in (c) are compared with those for stochiometric (open circles) and non-stochiometric (solid triangles) glasses quenched from the melt to the normal conditions, where solid squares correspond to the extrapolation from the quenched glasses to *in situ* melt (see the text). All lines are guides to the eye

has $n \approx 1.46$–1.47), which is in good agreement with the extrapolations of the refraction index vs density dependence established in [23, 24]. This glass has unusually high stability at normal pressure, and upon heating it slowly transforms to the ordinary B_2O_3 melt at $T > 800$ K. In this respect, the densified B_2O_3 glass obtained by pressure-temperature quenching from a solid state relaxes to the ordinary glassy state at temperatures 300 to 350 K at normal pressure, whereas the densified glasses prepared by quenching from melt at $P < 6.5$ GPa lose their excessive density at 400 to 700 K. High stability of the high-density glass correlates with high thermal stability of the B_2O_3 II high-pressure phase at normal pressure, which also transforms to the B_2O_3 melt at $T \approx 800$ K without the transition to the more stable B_2O_3 I phase.

6. If we used non-hermetic containers (graphite, *h*-BN, thin-wall Pt or Ta ampoules) for the high temperature (> 1700 K) experiments under pressure, a partial oxygen leakage resulted in non-stochiometric composition of boron oxide. The composition of the quenched glasses in this case varied from B_2O_3 to B_2O with most reproducible composition around $B_2O_{2.5}$ (see example of X-ray diffraction in Fig.2*d*). In *h*-BN and thin-wall Pt or Ta ampoules oxygen leakage at heating occurs at $P > 5.5$ GPa, as in graphite containers it occurs at $P > 1.5$ GPa. Rapid quenching of the non-stochiometric oxygen-depleted melt results in formation of high-density glass with the density of 2.8 to 2.95 g/cm^3 and index of refraction of 1.62 to 1.65 in a wide region of synthesis pressure from 1.5 to 7 GPa. This glass has rather high hardness $H \approx 9.5$ GPa in comparison to that of the ordinary glass ($H \approx 3$ GPa). At normal pressure this non-stochiometric high-density glass is unusually stable, it crystallizes at $T \approx 1100$ K to new modifications and decomposes with melting at $T \approx 1250$ K. The results of the detailed study of the structure and properties of the non-stochiometric high-density glasses and new boron oxide crystalline modifications will be presented elsewhere.

7. One can suppose that the high-density B_2O_3 glass and the corresponding liquid contain a large fraction of fourfold coordinated boron atoms. Therefore, at least two structural transformations should occur in liquid and possibly in glassy B_2O_3 under compression (Fig.4). The first diffuse transformation results in a decrease of the fraction of boroxol groups without noticeable changes in the first coordination spheres of B and O atoms. The second sharper transformations accompanies by drastic changes in the short-range coordinations of B and O atoms. The influence of the possible oxygen leakage for the second transition is not clear yet.

Thus, B_2O_3 is the first example of a substance, for which the *in situ* study was performed for both liquid and glassy state. The change of short-range order structure with the corresponding coordination increase

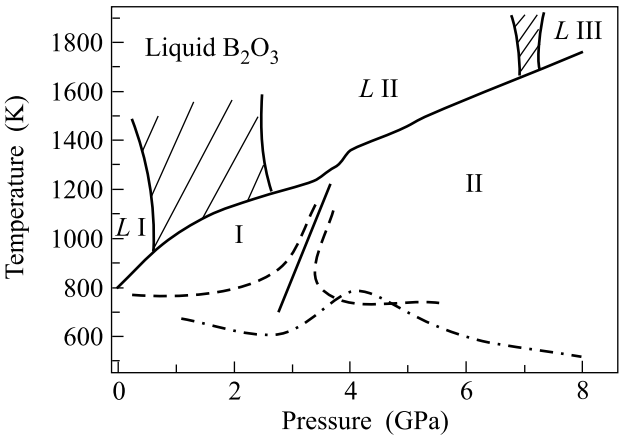

Fig.4. Approximate regions of transformations in liquid B_2O_3 mapped on the pressure-temperature phase diagram of B_2O_3 (see details in Fig.1)

seems to be general phenomenon for crystalline, liquid and glassy states. It would be of interest in the future to carry out *in situ* structural study of liquid B_2O_3 up to 10 GPa and glassy B_2O_3 up to 20 GPa to elucidate the high-pressure structural transformations and to acquire quantitative information about coordination changes. These investigations, as well as comprehensive study of the structure and properties of the high-density B_2O_3 glass are now in progress.

The authors are grateful to Dr. R. Sadykov and Dr. T. I. Duyzheva for the help in structural study, to N. V. Kalyaeva and A. V. Gulyutin for their assistance in the synthesis and density measurements, Dr. Yu. M. Tsipenyuk and Dr. B. A. Chapyzhnikov for the chemical analysis of the oxygen content in B_2O_3 samples, as well as to Prof. O. Shimomura and Prof. S. M. Stishov for helpful discussions. The work was supported by the Russian Foundation for Basic Research (Project # 01-02-16557 and # 02-02-16298) and by JAERI project, by JSPS.

1. *New Kinds of Phase Transitions: Transformations in Disordered Substances*, Eds. V. V. Brazhkin. S. V. Buldyrev, V. N. Ryzhov, and H. E. Stanley, NATO Science Series II: Mathematics, Physics and Chemistry – Vol. **81**, Kluwer, Dordrecht, 2002.
2. O. Mishima and Y. Suzuki, Nature **419**, 599 (2002).
3. Y. Katayama, private communication, Gordon Research Conference, Research at High Pressure, Meriden, NH, USA, June 23–28, 2002.
4. O. B. Tsiok, V. V. Brazhkin, A. G. Lyapin, and L. G. Khvostantsev, Phys. Rev. Lett. **80**, 999 (1998).
5. F. S. El'kin, V. V. Brazhkin, L. G. Khvostantsev et al., JETP Lett. **75**, 342 (2002).
6. J. Krong-Moe, J. Non. Cryst. Sol. **1**, 269 (1969).
7. G. E. Gurr, P. W. Montgomery, C. D. Knutson, and B. T. Gorres, Acta Cryst. **B26**, 906 (1970).
8. C. T. Prewitt and R. D. Shannon, Acta Cryst **B24**, 869 (1968).
9. J. D. Mackenzie and W. F. Claussen, J. Am. Ceram. Soc. **44**, 79 (1961).
10. F. Dachille and R. Roy, J. Am. Ceram. Soc **41**, 78 (1959).
11. D. R. Uhlmann, J. F. Hays, and D. Turnbull, Phys. Chem. Glass. **8**, 1 (1967).
12. J. Swenson and L. Borjesson, Phys. Rev. **B55**, 11138 (1997).
13. J. D. Mackenzie, J. Am. Ceram. Soc. **46**, 461 (1963).
14. A. C. Wright, C. E. Stone, R. N. Sinclair et al., Phys. Chem. Glass. **41**, 296 (2000).
15. E. Chason and F. Spaepen, J. Appl. Phys. **64**, 4435 (1988).
16. Th. Gerber, B. Himmel, and J. Weigelt, J. Non. Cryst. Sol. **126**, 35 (1990).
17. M. Misawa, J. Non. Cryst. Sol. **122**, 33 (1990).
18. J. Diefenbacher and P. F. McMillan, J. Phys. Chem. **A105**, 7973 (2001).
19. V. V. Brazhkin and A. G. Lyapin, J. Phys.: Condens. Matter, accepted for publication (2003).
20. M. Grimsditch, A. Polian, and A. C. Wright, Phys. Rev. **B54**, 152 (1996).
21. M. Grimsditch, R. Bhadra, and Y. Meng, Phys. Rev. **B38**, 4836 (1988).
22. K. Trachenko and M. T. Dove, J. Phys.: Condens. Matter **14**, 7449 (2002).
23. N. V. Surovtsev, J. Wiedersich, A. E. Batalov et al., J. Chem. Phys. **113**, 5891 (2000).
24. M. A. Ramos, J. A. Moreno, S. Vieira et al., J. Non. Cryst. Sol. **221**, 170 (1997).